Developing Spring-Roll Dielectric Elastomer Actuator System Based on Optimal Design Parameters

Medhat Awadalla[1] and Besada Anees[2]

[1] Communication, Electronics and Computers Department, Faculty of Engineering, Helwan University, Helwan, Egypt

[2] Communication, Electronics and Computers Department, Faculty of Engineering, Helwan University, Helwan, Egypt

Abstract

To develop a well designed practical spring-roll dielectric elastomer actuator system, we have to optimize its design parameters. In our pervious work, we have achieved the design parameters without taking the applied voltage required to activate the actuator into consideration because the applied voltage might change the optimal design parameters. In the paper, optimal design parameters have been achieved and decreased the applied voltage and the problems of high voltage are avoided. Furthermore, a voltage supply that is able to pump enough controlled charges to the actuator system is developed. A switched based multistage charge pump driven by a controlled low voltage switching power supply and a voltage driver is also proposed. The recently developed voltage supply is characterized by a wide range of controlled voltages. The achieved results based on the proposed approaches show that the design of the actuator is getting simpler and outperforms compared with the other related approaches.

Keywords: *Spring roll dielectric elastomer actuator, modes of failure, optimal design parameters, switching power supply, charge pump.*

1. Introduction

Dielectric elastomer actuators have been intensely studied in the recent decade. To explore some of the basic issues in the design, one particular type of actuators is studied, the spring-roll actuators [1-3]. The construction of a spring-roll actuator is sketched in Fig. 1. Two membranes of a dielectric elastomer are alternated with two electrodes. The laminate is prestretched in two directions in the plane, and then rolled around a spring [4, 5].

Two membranes of a dielectric elastomer are alternated with two electrodes. The laminate is first prestretched and then rolled around a relaxed spring. When the spring roll is subject to a voltage and an axial force, the length of the spring couples the electrical and mechanical actions.

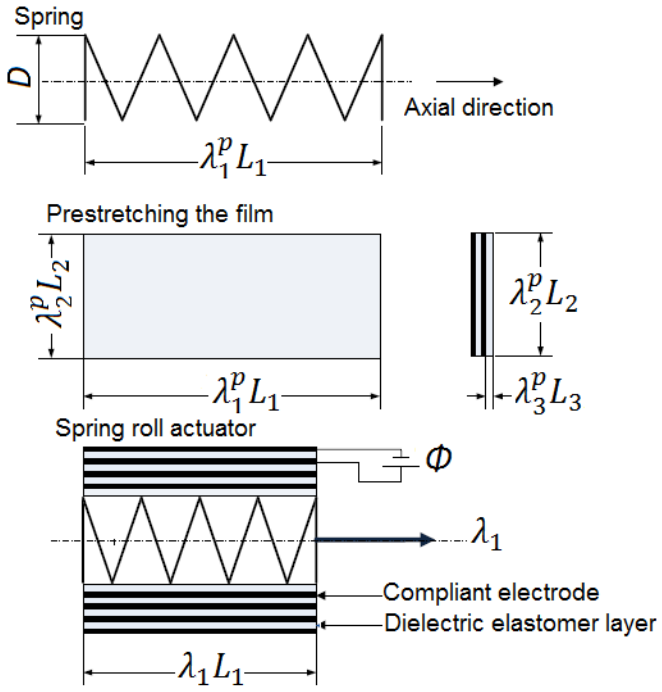

Fig. 1 The construction of a spring-roll dielectric elastomer actuator

When the actuator is subjected to an applied voltage and an applied axial force, the axial elongation couples the electrical and mechanical actions. The parameters of design include prestretches of the elastomer and the stiffness of the spring.

The continuation of the paper is as follows: Equations of state are derived in section 2. Modes of failure are illustrated in section 3. A new concept of actuation range is introduced in section 4. Optimal design parameters, design approaches and samples of actuator design are presented in section 5. Actuator system voltage supply is proposed in section 6. Section 7 gives the conclusion and future work

2. Equations of State

As shown in Fig. 1, the electrodes are compliant and bear no mechanical load. The elastomer has thickness L_3 and sides L_1 and L_2. The relaxed spring has a length $\lambda_1^p L_1$. The elastomer is prestretched to $\lambda_2^p L_2$ and $\lambda_1^p L_1$, and then the elastomer is rolled around the relaxed spring. When the actuator is subjected to an applied voltage Φ and an axial force *P*, the thickness of the laminate changes to $\lambda_3 L_3$, and the length of the spring changes to $\lambda_1 L_1$. However side 2 of the laminate, $\lambda_2^p L_2$, is constrained by the diameter of the spring and remains unchanged. The elastomer is taken to be incompressible, so that $\lambda_1\lambda_2^p\lambda_3 = 1$.

During the operation, the actuator varies its state in two ways, as specified by two generalized coordinates: the stretch λ_1 in the axial direction, and the charge *Q* on one of the electrodes. Helmholtz free energy *A* of the actuator is prescribed as a function of the two generalized coordinates:

$$A(\lambda_1, Q) = \frac{\mu}{2}\left(\lambda_1^2 + \left(\lambda_2^p\right)^2 + \left(\lambda_1\lambda_2^p\right)^{-2} - 3\right)L_1L_2L_3$$

$$+\frac{1}{2\varepsilon}\left(\frac{Q}{\lambda_1 L_1 \lambda_2^p L_2}\right)^2 L_1L_2L_3 + \frac{1}{2}K\left(\lambda_1 L_1 - \lambda_1^p L_1\right)^2 \qquad (1)$$

The free energy of the elastomer is the sum of the elastic energy, with μ being the shear modulus of the elastomer and the dielectric energy, with ε being the permittivity of the elastomer [6, 7]. The spring is taken to obey Hooke's law, with *k* being the stiffness of the spring.

When the actuator is in a state (λ_1, Q), in equilibrium with the applied axial force *P* and the applied voltage Φ, for any small change in the stretch and charge, $d\lambda_1$ and dQ, the change in the Helmholtz free energy equals the work done by the applied force and the voltage, namely [8].

$$dA = PL_1 + \Phi dQ \qquad (2)$$

Consequently, the force and the voltage are the partial differential coefficients of the free-energy function $A(\lambda_1, Q)$. The axial force is work-conjugate to the elongation:

$$P = \frac{\partial A(\lambda_1, Q)}{L_1 \partial \lambda_1} \qquad (3)$$

The voltage is work-conjugate to the charge:

$$\Phi = \frac{\partial A(\lambda_1, Q)}{\partial Q} \qquad (4)$$

Inserting (1) into (3), we can get:

$$\frac{P}{\mu L_2 L_3} = \left(\lambda_1 - \lambda_1^{-3}\left(\lambda_2^p\right)^{-2}\right) - \frac{1}{\lambda_1^3\left(\lambda_2^p\right)^2}\left(\frac{Q}{\sqrt{\mu\varepsilon}L_1L_2}\right)^2 + \alpha\left(\lambda_1 - \lambda_1^p\right) \qquad (5)$$

where $\alpha = \frac{KL_1}{\mu L_2 L_3}$ is a dimensionless ratio between the stiffness of the spring and that of the elastomer. Equation (5) shows that the axial force is balanced by contributions of three origins: the elasticity of the elastomer, the permittivity of the elastomer, and the elasticity of the spring. Equation (5) can also be obtained by invoking the Maxwell stress [9, 10].

Inserting (1) into (4), we obtain that

$$\frac{\Phi}{L_3}\sqrt{\frac{\varepsilon}{\mu}} = \frac{1}{\left(\lambda_1\lambda_2^p\right)^2}\left(\frac{Q}{\sqrt{\mu\varepsilon}L_1L_2}\right) \qquad (6)$$

The actuator has three dimensionless parameters: the prestretches in the two directions in the plane of the elastomer, λ_1^p and λ_2^p, as well as the normalized stiffness of the spring α. These parameters of design are prescribed once the actuator is constructed.

Equations (5) and (6) are the equations of state, relating the dimensionless loading parameters, $P/(\mu L_2 L_3)$ and $\Phi/\left(L_3\sqrt{\mu/\varepsilon}\right)$, to the dimensionless generalized coordinates, λ_1 and $Q/\left(L_1L_2\sqrt{\varepsilon\mu}\right)$.

These nonlinear equations of state can be displayed graphically on a plane spanned by the two dimensionless generalized coordinates as shown in Fig. 2. Plotted on this plane are the lines of constant force and the lines of constant voltage. Fig. 2 can be used to locate the state of the actuator under prescribed axial forces ($P/\mu L_2 L_3 = 0$, $P/\mu L_2 L_3 = -2$, and $P/\mu L_2 L_3 = -4$) and voltages ($\Phi/L_3\sqrt{\mu/\varepsilon} = 0.07$, $\Phi/L_3\sqrt{\mu/\varepsilon} = 0.1$, and $\Phi/L_3\sqrt{\mu/\varepsilon} = 0.2$). Plotting the equations of state in Fig. 2, we have set the parameters of design to a particular set of values.

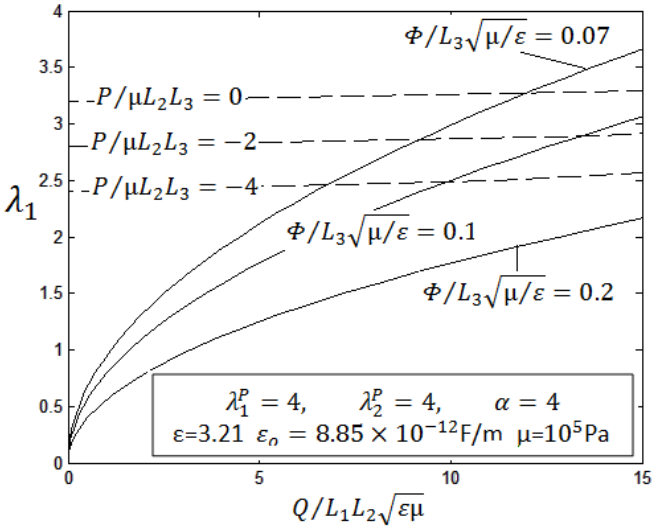

Fig. 2 A graphical representation of the equations of state

When the design variables $(\lambda_1^p, \lambda_2^p, and\ \alpha)$ are prescribed, the state of the actuator is characterized by two generalized coordinates: the stretch λ_1 in the axial direction, and the charge Q on one of the electrode.

3. Modes of Failure

The range of operation of an actuator is limited by various modes of failure. Each mode of failure restricts the state of the actuator to a region on the plane of the generalized coordinates. The common region that averts all modes of failure constitutes the set of allowable states. To illustrate the procedure to construct the region of allowable states, several representative modes of failure are considered [11, 12].

First *electromechanical instability* (EMI) of the elastomer is considered. When the applied voltage is increased, the elastomer reduces its thickness, so that the voltage induces a high electric field. The positive feedback between a thinner elastomer and a higher electric field may cause the elastomer to be reduced drastically, resulting in an electrical breakdown. This electromechanical instability can be analyzed by using a standard method in thermodynamics. [13].

Consider a three-dimensional space, with the generalized coordinates λ1 and Q being the horizontal axes, and the Helmholtz free energy A being the vertical axis. In this case, the free-energy function $A(\lambda_1, Q)$ is a surface. A point on the surface represents a state of the actuator, and a curve on the surface represents a path of actuation. Imagining a plane tangent to the surface at a state (λ_1, Q). The slopes of this tangent plane are $PL1$ and Φ, according to (3) and (4).

For a state (λ_1, Q) to be stable against arbitrary small perturbations in the generalized coordinates, the surface $A(\lambda_1, Q)$ must be convex at the point (λ_1, Q). This condition of stability is equivalent to the following set of inequalities:

$$\frac{\partial^2 A(\lambda_1, Q)}{\partial \lambda_1^2} > 0 \qquad (7a)$$

$$\frac{\partial^2 A(\lambda_1, Q)}{\partial Q^2} > 0 \qquad (7b)$$

$$\frac{\partial^2 A(\lambda_1, Q)}{\partial \lambda_1^2} \cdot \frac{\partial^2 A(\lambda_1, Q)}{\partial Q^2} > \left(\frac{\partial^2 A(\lambda_1, Q)}{\partial \lambda_1 \partial Q} \right)^2 \qquad (7c)$$

Based on the three inequalities, (7a) ensures mechanical stability, (7b) electrical stability, and (7c) electromechanical stability. Using (1), it is noticeable that (7a) and (7b) are satisfied for all values of (λ_1, Q), but (7c) is violated for some values of (λ_1, Q). A combination of (1) and (7c) shows that the electromechanical instability sets when:

$$\frac{Q}{\sqrt{\mu\varepsilon} L_1 L_2} = \sqrt{(1+\alpha)\lambda_1^4 (\lambda_2^p)^2 + 3} \qquad (8)$$

This equation corresponds to the curve marked by EMI in Fig. 3. The curve divides the (λ_1, Q) plane into two regions. Above the curve, the actuator is stable against small perturbation of the generalized coordinates. Below the curve, the actuator undergoes electromechanical instability.

The second mode of failure is the *electrical breakdown* (EB) of the elastomer. Even before the electromechanical instability sets, the electric field in the elastomer may become too high, leading to localized conduction path through the thickness of the elastomer. For the complexity of the microscopic process of electrical breakdown, it will not be addressed in this paper. To illustrate the procedure of design, we assume that electrical breakdown occurs when the true electric field exceeds a critical value *Ec*. For the ideal dielectric elastomer, $D = \varepsilon E$, where the true electric displacement is $D = Q/\lambda_1 \lambda_2^p L_1 L_2$, the condition for electric breakdown is

$$\frac{Q}{\sqrt{\mu\varepsilon} L_1 L_2} = \lambda_1 \lambda_2^p E_C \sqrt{\frac{\varepsilon}{\mu}} \qquad (9)$$

Equation (9) corresponds to the straight line marked by EB on the (λ_1, Q) plane as shown in Fig. 3. The actuator in a state in the region above this straight line will not suffer from the electrical breakdown.

Loss of tension of the elastomer when large voltage Φ is considered, or axial force P is compressive and of a large magnitude, the stress in the plane of the elastomer may cease to be tensile. This loss of tension will cause the elastomer to buckle out of the plane, so that elastomer will no longer generate force of actuation. To avert this mode of failure, the stress is required to be tensile in every direction in the plane of the elastomer. That is, both the stress along the axial direction and the stress in the circumferential direction are required to be tensile, $S_1 > 0$ and $S_2 > 0$. Following [14], the nominal stress in the axial direction is obtained in terms of the two generalized coordinates:

$$\frac{S_1}{\mu} = \left(\lambda_1 - \lambda_1^{-3} (\lambda_2^p)^{-2} \right) - \left(\frac{Q}{\sqrt{\mu\varepsilon} L_1 L_2} \right)^2 \lambda_1^{-3} (\lambda_2^p)^{-2} \qquad (10)$$

Setting the critical condition in (10), we obtain that

$$\frac{Q}{\sqrt{\mu\varepsilon} L_1 L_2} = \sqrt{\lambda_1^4 (\lambda_2^p)^2 - 1} \qquad (10a)$$

Similarly, nominal stress s_2 in terms of the two generalized coordinates can be obtained:

$$\frac{S_2}{\mu} = \left(\lambda_2^p - (\lambda_2^p)^{-3} \lambda_1^{-2} \right) - \left(\frac{Q}{\sqrt{\mu\varepsilon} L_1 L_2} \right)^2 (\lambda_2^p)^{-3} \lambda_1^{-2} \qquad (11)$$

Setting the critical condition s_2=0 in (11), the following equation can be obtained:

$$\frac{Q}{\sqrt{\mu\varepsilon} L_1 L_2} = \sqrt{\lambda_1^2 (\lambda_2^p)^4 - 1} \qquad (11a)$$

The critical conditions for loss of tension, s_1=0 and s_2=0, are plotted in Fig. 3. A comparison of (8) and (10a) shows that, for spring-roll actuators, loss of tension in the axial direction will always precede electromechanical instability. In contrary, other types of dielectric elastomer actuators may fail by electromechanical instability [15, 16].

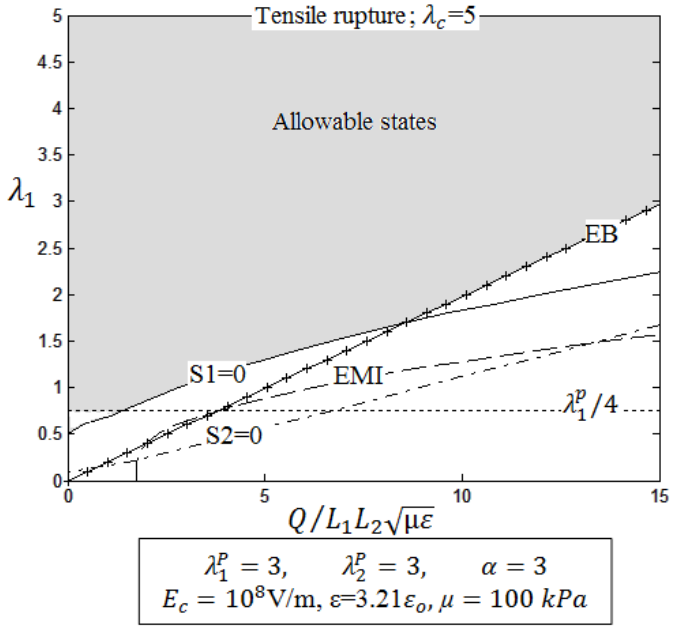

Fig. 3 A graphical representation of modes of failure

Next *tensile rupture* of the elastomer is considered. When an elastomer is stretched too severely, the elastomer may rupture. The critical condition for tensile rupture is not well quantified. Here the simple criterion that the elastomer will rupture when either stretch, λ_1 or λ_2 exceeds a critical value λ_c is used. A representative value λ_c = 5 is included in Fig.3.

The *compressive limit* of the spring is finally considered. The spring in the spring-roll actuator is designed to be under compression. When the spring is compressed excessively, however, it may deform plastically. The length of the spring at its relaxed state is $\lambda_1^p L_1$, and the length of the actuated spring is $\lambda_1 L_1$. We assume that the spring deforms plastically when λ_1^p/λ_1 exceeds a critical value *c*, which we set to be *c* = 4. In the (λ_1, Q) plane, Fig. 3, the region above the line $\lambda_1 = \lambda_1^p/c$ will guarantee that the spring remains elastic.

The modes of failure discussed in this section are all averted in the shaded region in Fig. 3. As evident from the above discussion, this region of allowable states will depend on the critical conditions for various modes of failure.

4. Actuation Range

The actuation range is an important issue because the applied voltage may take different values within the actuation range.
In this paper the concept of actuation range depends upon whether the actuator has a fixed load actuator or variable multi-load actuator. The fixed load actuator is the actuator subject to a fixed axial force (i.e., a dead weight). In this case the actuation range is very small value starting at the state of zero charge, and ending at the state where the line of a failure mode intersects the axial force line. Fig. 4 shows the actuation range for a fixed load actuator. The actuation range extends from $\lambda_1 = 4.4$ to $\lambda_1 = 4.515$ (the two highlighted black points) when $\lambda_1^p = 5$, $\lambda_2^p = 5$, $\alpha = 10$, $P/\mu L_2 L_3 = -1$, and $E_C = 10^8 v/m$.

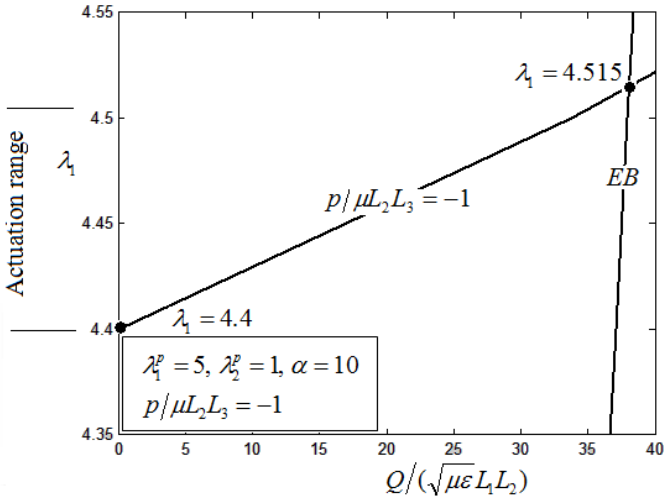

Fig. 4 The actuation range for a fixed load actuator when $\lambda_1^p = 5$, $\lambda_2^p = 5$, $\alpha = 10$, $P/\mu L_2 L_3 = -1$, and $E_C = 10^8 v/m$.

The load of the exchangeable multi-load actuator can be replaced by another unequal load and this load in turn can be replaced by another unequal one and so on. The actuation range of the exchangeable multi-load actuator starts at the state of zero charge of heaviest load and ends at the state where the line of a failure mode intersects the line of the lightest load. Fig. 5 shows the actuation range of the exchangeable multi-load actuator. The actuator given in fig. 5 subjects to one of the following dimensionless loads ; $P/\mu L_2 L_3 = -1$, $P/\mu L_2 L_3 = -10$, $P/\mu L_2 L_3 = -20$, or $P/\mu L_2 L_3 = -30$. The actuation range in this case starts at $\lambda_1 = 1.95$ and ends at $\lambda_1 = 4.52$ (the two highlighted black points).

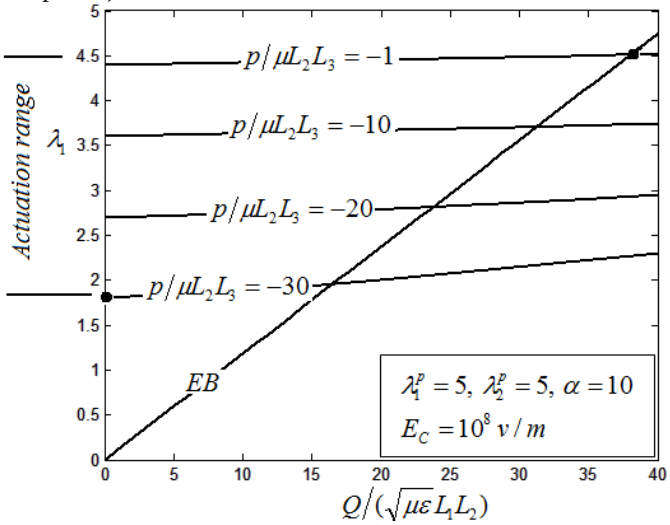

Fig. 5 The actuation range of the exchangeable multi-load actuator

5. Spring-Roll Dielectric Elastomer Actuator Design

Parameters of design are prescribed once the actuator is constructed therefore they must well studied and selected to be optimal.

5.1 Spring-Roll Dielectric Elastomer Actuator Optimal Design Parameter

To optimize an actuator, the actuator should have certain features such as higher actuation and the ability to burden heavier loads. To address this issue, we have to figure out the space of design parameters values that confirm these features.

Spring-roll dielectric elastomer optimal design parameters according to [17] are $\lambda_1^p = 5,\ \lambda_2^p = 2,\ \alpha = 10$. These parameters of design are prescribed once the actuator is constructed.

In this paper we will address the effect of λ_2^p on actuation λ_1, axial force $P/\mu L_2 L_3$, and $\Phi/\left(L_3\sqrt{\mu/\varepsilon}\right)$ to prove that the value $\lambda_2^p = 2$ that was considered as an optimal value should be changed to $\lambda_2^p = 5$.

The actuation λ_1 as a function of λ_2^p

The obtained results in simulation show that when λ_2^p increases, the actuation λ_1 slightly decreases. There is no big difference between actuation at $\lambda_2^p = 1$ and actuation at $\lambda_2^p = 5$ even at higher values of the dimensionless charge. From fig. 6, it is clear that λ_2^p slightly affects λ_1.

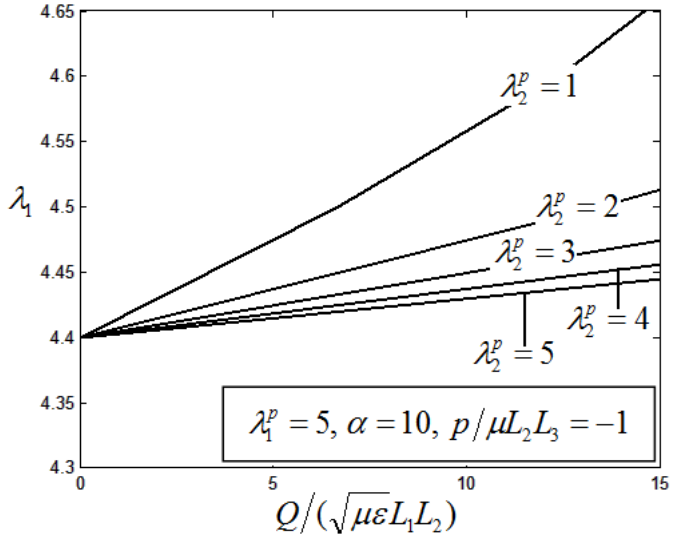

Fig. 6 The effect of λ_2^p on the actuation λ_1 at $\lambda_1^p = 5,\ \alpha = 10,\ and\ P/\mu L_2 L_3 = -1$

The dimensionless force (load) $P/\mu L_2 L_3$ as a function of λ_2^p

The dimensionless axial force $P/\mu L_2 L_3$ is a nonlinear function of λ_2^p . λ_2^p slightly affects the value (modulus) of the axial force. Fig. 7 shows the effect of λ_2^p on the axial force.

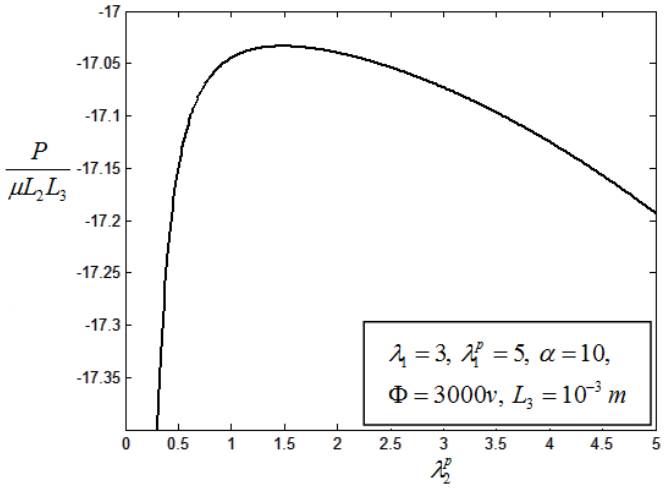

Fig. 7 The effect of λ_2^p on the axial force $P/\mu L_2 L_3$ at $\lambda_1 = 3,\ \lambda_1^p = 5,$ $\alpha = 10,\ L_3 = 10^{-3},$ and $\Phi = 3000v$

The effect of λ_2^p on the applied voltage Φ

λ_2^p Slightly affects both actuation λ_1 and dimensionless axial load $p/\mu L_2 L_3$ but it has a great effect on the applied voltage Φ. When the applied voltage decreases, λ_2^p will increase. Let us take the applied voltage at a critical state Φ_C where one failure mode sets in as an example for the relation between the applied voltage and λ_2^p . When $\lambda_1^p = 5,\ \lambda_2^p = 1,\ \alpha = 10,$ $p/\mu L_2 L_3 = 0,\ and\ L_3 = 1mm$, the critical dimensionless applied voltage is 0.215 and the critical applied voltage is $12756\ v$, as shown in fig. 8.

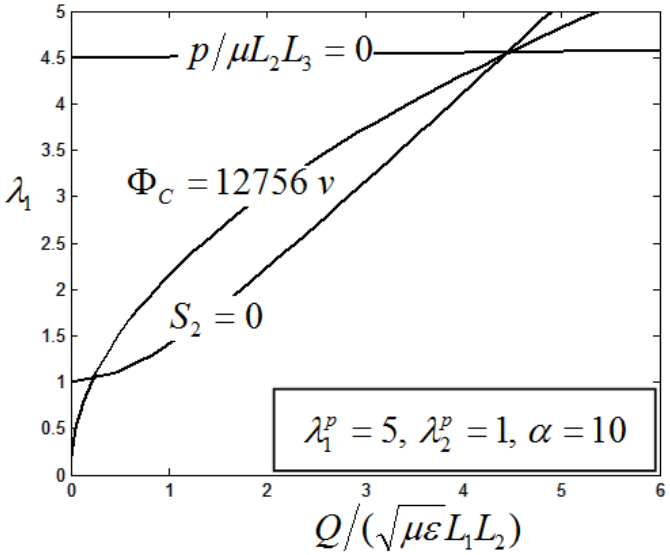

Fig. 8 Critical applied voltage at $\lambda_1^p = 5,\ \lambda_2^p = 1,\ \alpha = 10,$ $p/\mu L_2 L_3 = 0,\ and\ L_3 = 1mm$

When $\lambda_1^p = 5,\ \lambda_2^p = 2,\ \alpha = 10,\ p/\mu L_2 L_3 = 0,\ and\ L_3 = 1mm$, the critical dimensionless applied voltage is 0.182 and the critical applied voltage is $10798v$, look at fig. 9.

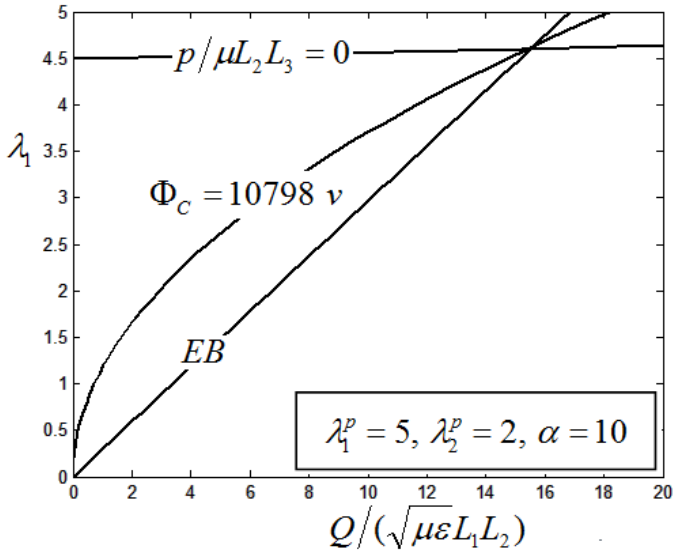

Fig. 9 Critical applied voltage at $\lambda_1^p = 5,\ \lambda_2^p = 2,\ \alpha = 10,$ $p/\mu L_2 L_3 = 0,\ and\ L_3 = 1mm$

When $\lambda_1^p = 5,\ \lambda_2^p = 3,\ \alpha = 10,\ p/\mu L_2 L_3 = 0,\ and\ L_3 = 1mm$, the critical dimensionless applied voltage is 0.122 and the critical applied voltage is $7238v$, as shown in fig. 10.

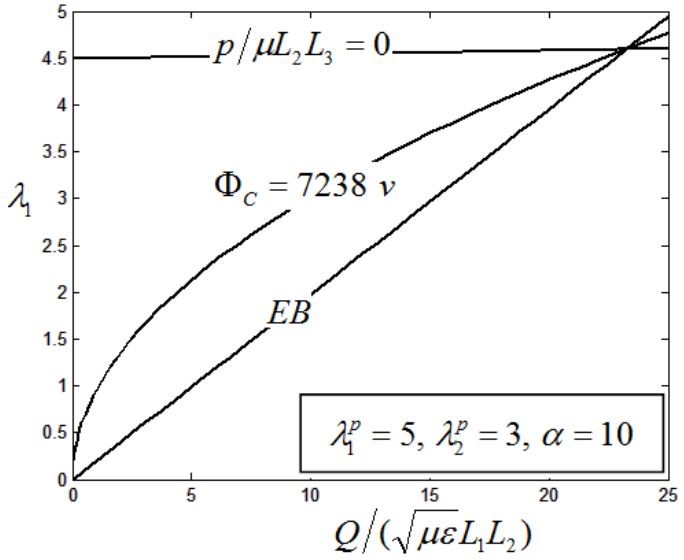

Fig. 10 Critical applied voltage at $\lambda_1^p = 5,\ \lambda_2^p = 3,\ \alpha = 10,$ $p/\mu L_2 L_3 = 0,\ and\ L_3 = 1mm$

When $\lambda_1^p = 5,\ \lambda_2^p = 4,\ \alpha = 10,\ p/\mu L_2 L_3 = 0,\ and\ L_3 = 1mm$, the critical dimensionless applied voltage is 0.092 and the critical applied voltage is $5458v$, look at fig. 11.

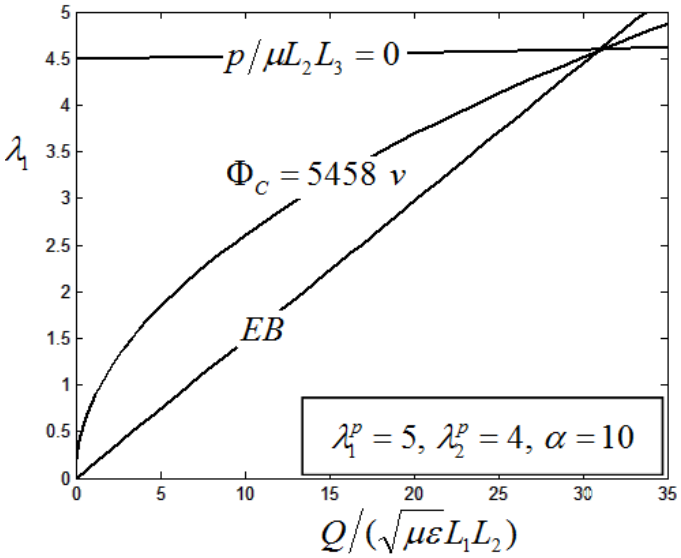

Fig. 11 Critical applied voltage at $\lambda_1^p = 5,\ \lambda_2^p = 4,\ \alpha = 10,$ $p/\mu L_2 L_3 = 0,\ and\ L_3 = 1mm$

When $\lambda_1^p = 5,\ \lambda_2^p = 5,\ \alpha = 10,\ p/\mu L_2 L_3 = 0,\ and\ L_3 = 1mm$, the critical dimensionless applied voltage is 0.073 and the critical applied voltage is $4331v$, look at fig. 12.

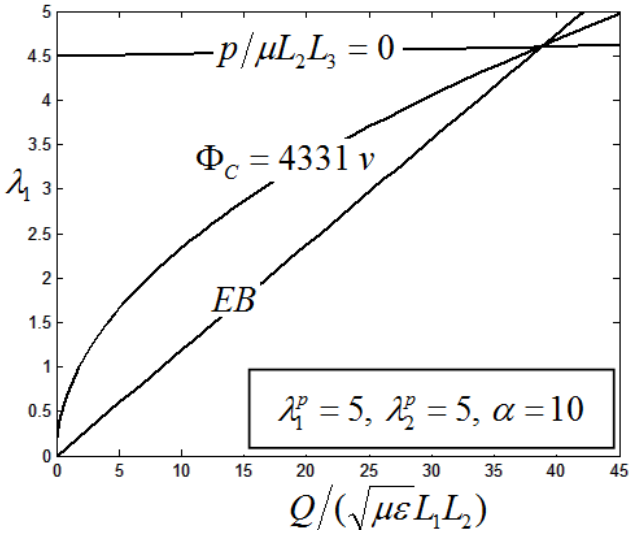

Fig. 12 Critical applied voltage at $\lambda_1^p = 5,\ \lambda_2^p = 5,\ \alpha = 10,$ $p/\mu L_2 L_3 = 0,\ and\ L_3 = 1mm$

The voltage at a critical state Φ_C decreases from 12756v at $\lambda_2^p = 1$ to 4331v at $\lambda_2^p = 5$. In general, the applied voltage decreases as λ_2^p increases and high voltage problems can be avoided therefore the optimal design parameters should be changed from;

$$\lambda_1^p = 5,\ \lambda_2^p = 2,\ \alpha = 10$$

to:

$$\lambda_1^p = 5,\ \lambda_2^p = 5,\ \alpha = 10$$

5.2 Spring-Roll Dielectric Elastomer Actuator Optimal Design Parameters

Spring-roll dielectric elastomer actuator is designed according to equations of state (eq. 5, and eq. 6). The first step of designing the elastomer actuator is to be aware of the constant values of equations of state;

μ : The shear modulus of the dielectric elastomer (VHB 4910 material) equals $10^5 Pascal$ [18].

ε_r : The relative dielectric constant equals 3.21 for VHB 4910 material, at a frequency of 1 KHz.

ε_o : The permittivity equals 8.85×10^{-12} Farad/meter.

E_C : The electric breakdown of VHB 4910 material equals $10^8 v/m$.

λ_1^p , λ_2^p , α : The design parameters are dealt as constant values; $\lambda_1^p = 5,\ \lambda_2^p = 5,\ \alpha = 10$.

L_3 : The thickness of the dielectric elastomer (VHB 4910 material), 3M company produces it in a thickness of 1 mm therefore it is dealt as a constant value.

Spring-roll dielectric elastomer specifications prescribed by the customer

The customer has to specify three specifications before the actuator is constructed; axial force/forces in Newtons, length of the actuator at relax $L_{1\ relax}$ in meters, and actuator maximum required length $L_{1\max}$ in meters. Dimensionless axial force/forces should not be positive (tensile force/forces) and should not situate in the region of modes of failure. If this happens, the customer is reviewed to modify his request.

Determining the maximum actuation (stretch) $\lambda_{1\max}$

$$L_{1\ relax} = \lambda_1^p L_1$$
$$L_{1\max} = \lambda_{1\max} L_{1\ relax}$$
$$\lambda_{1\max} = L_{1\max} / L_{1\ relax}$$

Determining the range of the applied voltage

The applied voltage may take infinite different values along the actuation range starting at $\Phi = 0$ and ending at $\Phi = \Phi_C$. $E = \Phi/\lambda_3 L_3$ where E is the electric field across the elastomer membrane. When $\Phi = \Phi_C$, $E = E_C$, where E_C is the electric breakdown field. Then $E_C = \Phi_C/\lambda_3 L_3$. Since the dielectric elastomer is incompressible material, $\lambda_3 = 1/(\lambda_2^p \lambda_1)$.

$$\Phi_C = \frac{10^8 L_3}{\lambda_2^p \lambda_1} \quad (12)$$

where;

$E_C = 10^8 v/m$ for VHB 4910 dielectric elastomer material.

λ_2^p according to new derived optimal design parameters equals "5".

3 M company produces VHB 4910 membrane in a thickness of 1 mm. Φ_C can be determined.

Determining L_2 , the width of the elastomer membrane

Substituting $\lambda_{1\max}$ *and* Φ_C in eq. 6, dimensionless charge $Q/(\sqrt{\mu\varepsilon} L_1 L_2)$ can be determined. Substituting the determined $Q/(\sqrt{\mu\varepsilon} L_1 L_2)$ and $\lambda_{1\max}$ in eq. 5, L_2 can be determined.

Determining *K*, the stiffness of the spring

$L_1 = L_{1\ relax}/\lambda_1^p$, L_2 has been determined in section 6.4. Substituting L_1 *and* L_2 in the following eq; $\alpha = KL_1/\mu L_2 L_3$, K can be determined.

Determining *n*, number of turns of actuator membrane around the spring

Approximately the number of turns of the actuator membrane can be determined by dividing the width of the actuator L_2 by the circumference of the spring.

$$n = \frac{\lambda_2^p L_2}{2\pi r} \quad (13)$$

where; r is radius of the used spring.

5.3 Samples of Spring-Roll Dielectric Elastomer Design Results

In appendix A we develop equations of state based on Mat-Lab program help design spring-roll dielectric elastomer actuators. The customer has to specify the relaxed length of the actuator $L_{1\ relax}$, the maximum required length the actuator has to achieve $L_{1\max}$, and axial load the actuator will treat with.

Table 1: Samples of spring-roll dielectric elastomer design specifications

p	L_{1relax}	$L_{1\max}$	r	L_1	L_2	L_3	Φ_c	$\lambda_{1\max}$	k	n
-4	0.01	0.02	0.001	0.02	0.0014	0.001	10000	2	679.7	1.08
-8	0.02	0.05	0.001	0.004	0.0034	0.001	8000	2.5	846	2.7

-12	0.03	0.09	0.001	0.006	0.0067	0.001	6667	3	1114	5.3
-16	0.04	0.14	0.0025	0.008	0.013	0.001	5714	3.5	1624	4.14
-20	0.05	0.05	0.0025	The actuator is overloaded						
-24	0.06	0.07	0.0025	The actuator is overloaded						
+28	0.07	0.14	0.0025	The load is a tensile forces						
+32	0.08	0.184	0.0025	The load is a tensile force						
-36	0.09	0.225	0.005	0.0180	0.0152	0.001	8000	2.5	846	2.4
-40	0.1	0.29	0.005	0.02	0.021	0.001	6897	2.9	1048	3.3
-44	0.11	0.352	0.005	0.022	0.028	0.001	6250	3.2	1274	4.5
-48	0.12	0.42	0.005	0.024	0.039	0.001	5714	3.5	1624	6.2
-52	0.13	0.234	0.005	0.026	0.0164	0.001	11111	1.8	629	2.6
-56	0.14	0.294	0.005	0.028	0.0198	0.001	9524	2.1	708	3.2
-60	0.15	0.345	0.005	0.03	0.231	0.001	8696	2.3	771	3.7
-64	0.16	0.432	0.005	0.032	0.03	0.001	7407	2.7	937	4.8
-68	0.17	0.527	0.005	0.034	0.0404	0.001	6452	3.1	1189	6.4
-72	0.18	0.702	0.005	0.036	0.092	0.001	5128	3.9	2555	14.6
-76	0.19	0.76	0.01	0.038	0.1132	0.001	5000	4	2980	9
-80	0.2	0.82	0.01	0.04	0.143	0.001	4878	4.1	3576	11.4
-84	0.21	0.399	0.01	0.042	0.0275	0.001	10526	1.9	654	2.2
-88	0.22	0.484	0.01	0.044	0.0325	0.001	9090	2.2	738	2.6
-92	0.23	0.598	0.01	0.046	0.0409	0.001	7692	2.6	889	3.3
-96	0.24	0.576	0.01	0.048	0.0387	0.001	8333	2.4	807	3.1
+100	0.25	0.975	0.01	The load is a tensile force						

Using the above mentioned software, we can design actuator specifications; the dimensions of the actuator membrane, the stiffness of the used spring, the maximum applied voltage, and maximum achieved actuation. Table 1 includes samples of design specifications where the dimensions $L_1, L_2, L_3, L_{1\max}, L_{1relax}, and\ r$ are measured in *meters*, $\Phi_{\max}$ *or* $\Phi_{critical}$ is measured in volts, stiffness of the spring k is measured in *newtons per meter*, and the axial load p is measured in *newtons*.

6. Spring-Roll Dielectric Elastomer Actuator Voltage Supply

In spring-roll dielectric elastomer actuator system to achieve a specific actuation λ_1, a specific voltage should be applied to the electrodes of the actuator and specific charges should flow to them, therefore a voltage supply whose output ranges from several volts up to $15000\,v$ is required. This voltage supply should be adjusted automatically to any voltage between 0 and 15000v whatever the value of the required voltage is.

A charge pump driven by a low voltage switching power supply and a voltage drive is presented in this paper [19].

6.1 Charge Pump

Increased voltage levels are obtained in a charge pump as a result of transferring charges to a capacitive load and do not involve amplifiers or transformers. The charge pump is constructed by n cascaded voltage doublers. Charge pump operates by switching on and off a large number of switches which charge and discharge a large number of capacitances, transferring energy to the output load. Switched-capacitor charge pumps have exponentially growing voltage gain as a function of the number of stages (voltage doublers) up to 2^n [20].

A switched-capacitor organization of a two phase DC-DC voltage doubler is shown in Fig. 13. It contains 2 clock controlled switches and 2 capacitors.

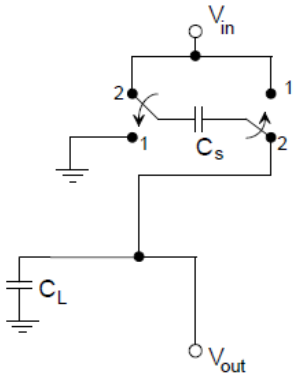

Fig. 13 The DC-DC TPVD voltage doubler

For a simple explanation of the voltage doubler operation, let us assume that the switches and capacitors are all ideal. That is, we assume that there is no leakage current in capacitors, switches dissipate no energy and the electric charge transferring is instantaneous. Fig. 14.a shows the equivalent circuit of the voltage doubler when the circuit is in the *Kth* iteration cycle and the clock is in phase 1. At this time instance, the load capacitor C_L holds the previous voltage value.

$$V_{out}^{[K]} = V_{out}^{[K-1]} \quad (14)$$

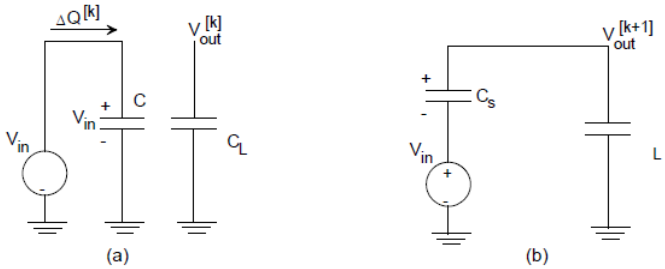

Fig. 14 The equivalent circuits in two clock phases.

The voltage across the capacitor C_S changes from $-(V_{in} - V_{out}^{[K-1]})$ to V_{in}. The charge $\Delta Q^{[K]}$ transferred from the voltage source V_{in} to C_S is obtained from

$$\Delta Q^{[K]} = C_S\left(V_{in} - \left(-\left(V_{in} - V_{out}^{[K-1]}\right)\right)\right) = C_S\left(2V_{in} - V_{out}^{K}\right) \quad (15)$$

Equation (15) implies that the voltage source *Vin* would stop transferring charge to C_S if $V_{out}^{[K]} = 2V_{in}$.

Fig. 14.b shows the equivalent circuit of the voltage doubler when the circuit is in the $(k+1)th$ iteration cycle and the clock is in phase 2. According to the charge conservation law at the node connecting C_S and C_S, and evaluating charges stored in capacitors as $Q = C\,V$, the relationship between voltages at $k\,th$ and $(k+1)th$ iteration can be expressed by

$$V_{in} \times C_S + V_{out}^{[K]} \times C_L = \left(V_{out}^{[K+1]} - V_{in}\right) \times C_S + V_{out}^{[K+1]} \times C_L \quad (16)$$

If we set $r = \dfrac{C_S}{C_L + C_S}$, to represent the capacitor ratio, then

$$V_{out}^{[K+1]} = (1-r)V_{out}^{K} + 2rV_{in} \quad (17)$$

where $0 < r < 1$. Thus, V_{out} can be represented as a sequence of the iteration index *k*.

Fig. 15 shows the voltage gains *Av* as a function of the iteration index *k*, with different *r*. The smaller the *r*, the larger the ratio of the grounded capacitor C_L to the switched capacitor *Cs*. It is clear that the final (steady state) value of the voltage gain *Av* is 2 independently of the capacitor ratio *r*. That is, the circuit in Fig. 14 works as a voltage doubler provided that the voltage source V_{in} supplies enough charge to the charge pump. The larger C_L (smaller *r*) requires more clock cycles (bigger *k*) to reach the desired output voltage. The value of *r* does not influence the final voltage gain.

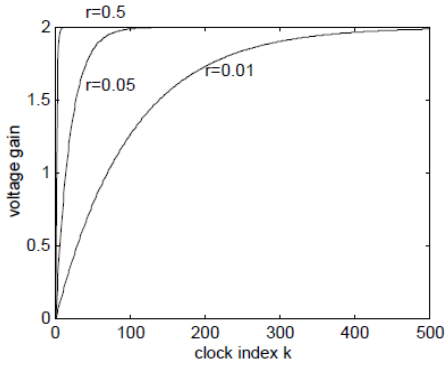

Fig. 15 The voltage gain as a function of the clock index *k*

6.2 Proposed Actuator Voltage Supply

A new organization of spring-roll dielectric elastomer actuator voltage supply is presented in this paper. Switched multistage charge pump driven by a controlled low voltage switching power supply and a voltage driver is used as a variable output high voltage supply. Coarse adjustment of the output voltage is automatically accomplished by connecting a specific number of the stages of the charge pump to the actuator. Fine adjustment of the output voltage is automatically accomplished by controlling the width of the pulse of the low voltage switching power supply. Fig. 16 shows the block diagram of the proposed voltage supply.

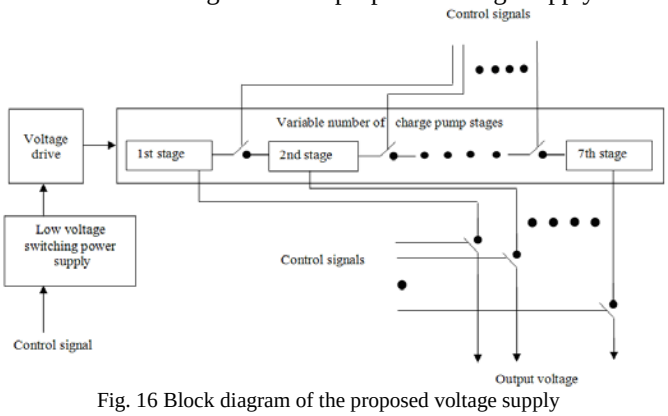

Fig. 16 Block diagram of the proposed voltage supply

The voltage driver is designed to supply 120 volt at a 50% duty cycle in the low voltage switching power supply. The input and output voltages of each stage of the charge pump are indicated in table 2.

Table 2: The input and output and output of each stage of the charge pump

Charge pump stage number	***Input voltage***	Output voltage
1	120	240
2	240	480
3	480	960
4	960	1920

5	1920	3840
6	3840	7680
7	7680	15360

At reset state all switches are switched off, duty cycle of low voltage switching power supply is 50% and the output of the voltage driver is 120 volt. Suppose that the actuator needs instantaneous 4000 volt to achieve a specific actuation, the control circuit connects stages umber 1, 2, 3, 4, and 5 in series and the output is taken from the fifth stage (the automatic coarse adjustment), then the control circuit increases the duty cycle (pulse width) of the voltage switching power supply until the output of the fifth stage reaches 4000 volt (the automatic fine adjustment).

7. Conclusion

In this paper we search two problems, the first is to develop an optimal design parameters based spring-roll dielectric elastomer actuator, and the second is to develop a controlled wide range output high voltage supply. As for the first problem, we prove that λ_2^p has slight effect on both actuation λ_1 and axial load, but has a high effect on the applied high voltage, it reduces the required applied high voltage down to 35% when raised to 5. Therefore the optimal design parameters are changed to; $\lambda_1^p = 5, \lambda_2^p = 5, \alpha = 10$.

In this paper we develop procedures of designing a spring-roll dielectric elastomer actuator, involve a software help designing the actuator [appendix 1], and mention samples of the results of designed spring-roll dielectric elastomer actuators.

In this paper the concept of actuation range depends upon whether the actuator is a fixed load actuator or an exchangeable multi-load actuator.

As for the second problem a switched multistage charge pump driven by a controlled low voltage switching power supply and a voltage driver is proposed as a wide range output high voltage supply.

Solving the two problems a complete spring-roll dielectric elastomer actuator system is developed.

For future work, the instantaneous change of actuation of the spring-roll dielectric elastomer actuator is required. This actuation can be controlled by controlling both charges pumped to the electrodes of the actuator and the voltage applied to them. In a next paper we shall develop a sub control system to control charges pumped to electrodes of the actuator and another sub control system to control the applied voltage. Modes of failure of the actuator will be avoided using the proposed control system. Sensors of charges and sensors of high voltage will be used. Intelligent system will be proposed.

Appendix A

```
function [l1, l2, d1max, phic, k, n]=actdesign (p, l1relax, l1max, r)
% We develop this equations of state based Mat-Lab program to design spring-roll
% dielectric elastomer actuators.
% l1max is the maximum required actuator length.
% l1relax is the spring-roll dielectric elastomer actuator at relax.
% p (lowr case letter)is the compressive load in Newtons.
% P (upper case letter) is the dimensionless axial force.
% phic is the applied voltage at a critical state.
% d1max is maximum actuation.
% r is the radius of spring.
% n number of turns of the actuator membrane around the spring.
% k is the stiffness of the spring.
% l1, l2 and l3 are the length, width and thickness of the actuator membrane.
% mu is the shear modulus of the actuator material (dielectric elastomer).
% epsilon is the dielctric of the actuator material.
% d1p & d2p are the prestretches in in the length and width of the
% membrane.
% Q (upper letter) is the dimensionless charge.
% Given (l1max, l1relax, and p), [l1, l2, d1max, phic, k]can be determined.
mu=10.^5;
epsilon=3.21*8.85*10.^-12;
d1p=5;
d2p=5;
a=10;
l3=10.^-3;
if p<0
   l1=l1relax/d1p;
   d1max=l1max/l1relax;
   phic=(10.^8*l3)/(d2p*d1max);
   Q=(d1max.^2)*(d2p.^2)*(phic/l3)*(sqrt(epsilon/mu));
   P=d1max - ((d1max.^-3)*(d2p.^-2)) - ((Q.^2)*(d1max.^-3)*(d2p.^-2)) + a*(d1max-d1p);
   if P>-35;
      l2=p/(P*mu*l3);
      k=(a*mu*l2*l3)/l1;
      n=(d2p*l2)/(2*pi*r);
   else
      disp ('The actuator is overloaded');
% The word "overloaded" means that the actuator may subjects to a failure mode.
      l1=[];
      l2=[];
      d1max=[];
      phic=[];
      k=[];
      n=[];
   end
else
```

```
    disp ('The Load is a tensile force');
  % The load should be a compressive load (-ve)and should
not be tensile (+ve).
  l1=[];
  l2=[];
  d1max=[];
  phic=[];
  k=[];
  n=[];
end
```

References

[1] Rui Zhang, Patrick Lochmatter, Andreas Kun and Gabor Kovacs, "Spring Roll Dielectric Elastomer Actuators for a Portable Force Feedback Glove," Proceedings of SPIE Vol. 6168, 61681T, (2006).
[2] Q. Pei, R. Pelrine, S. Stanford, R. Kornbluh, M. Rosenthal, Synthetic Metals, 135-136, 129-131(2003).
[3] Q. Pei, R. Pelrine, S. Stanford, R. Kornbluh, M. Rosenthal, K. Meijer, R. "Full, Smart Structures and Materials," Proc. of SPIE Vol. 4698, 246 (2002).
[4] Guggi Kofod, "The static actuation of dielectric elastomer actuators: how does pre-stretch improve actuation?," J. Physics. D: Appled Physics. 41 215405 (11pp) (2008)
[5] Woosang JUNG, Yutaka TOI, "Computational Modeling of Electromechanical Behaviors of Dielectric Elastomer Actuators," Proceedings of the International MultiConference of Engineers and Computer Scientists 2010 Vol III, IMECS 2010, March 17-19, 2010, Hong Kong.
[6] X. Zhao, W. Hong, Z. Suo, Physical review B 76 (2007).
[7] G. Kofod, M. Paajanen, S. Bauer, Applied Physics" a-Materials Science & Processing 85, 141(2006).
[8] Z. G. Suo, X. H. Zhao, and W. H. Greene, Journal of the Mechanics and Physics of Solids 56, 467-486 (2008).
[9] R. Zhang, P. Lochmatter, A. Kunz, G. Kovacs, Smart Structures and Materials, Proc. of SPIE Vol. 6168 (2006).
[10] G. Kovacs, P. Lochmatter, M. Wissler, Smart Materials and Structures, Vol. 16, S306-S317 (2007).
[11] R. E. Pelrine, R. D. Kornbluh, J. P. Joseph, Sensors and Actuators A 64, 77 (1998).
[12] J. S. Plante, S. Dubowsky, International Journal of Solids and Structures 43, 7727 (2006).
[13] A. N. Norris, Applied Physics Letters 92, 026101 (2008).
[14] X. Zhao, Z. Suo, Applied Physics Letters 91 (2007).
[15] Tianhu He, Xuanhe Zhao and Zhigang Suo, "Equilibrium and stability of dielectric elastomer membranes undergoing inhomogeneous deformation," School of Engineering and Applied Sciences, Harvard University, (2-10-2008).
[16] Christoph Keplinger, Martin Kaltenbrunner, Nikita Arnold, and Siegfried Bauer, Röntgen's electrode-free elastomer actuators without electromechanical pull-in instability,Applied physical science, (December 15, 2009).
[17] Medhat H. Ahmed and Besada A. Anees, "Parameter Optimization in Spring-Roll Dielectric Elastomer Actuator Design",The Journal of Engineering Sciences, Faculty of Engineering , University of Assiut, Assiut, Egypt, 2011.
[18] Mickael Moscardo, Xuanhe Zhao, Zhigang Suo,_ and Yuri Lapusta, "On designing dielectric elastomer actuators," Journal of Applied Physics 104, 093503, (2008).
[19] Sandeep Pemmaraju, "High voltage charge pump circuit for an ion mobility spectrometer", submitted for the degree of Master of science in Engineering, Electrical Engineering, Boise State University, 2004.
[20] Janusz A. Starzyk, Ying-Wei Jan, and Fengjing Qiu, "A DC-DC charge pump design based on voltage doublers" IEEE transactions on circuits and systems – I: fundamental theory and applications, vol. 48, no. 3, March 2001.

Medhat H A Awadalla obtained his B.Sc. degree from Helwan University in 1991 in the Electronics and Communications Department and his M.Sc in the field of reconfigurable computer architecture in 1996 from Helwan University. He received his PhD from Cardiff University, UK in the field of mobile robots in 2005. He was a postdoctoral fellow at Cardiff University in 2006 and currently he is working as an Assistant Professor in Helwan University. His research interests include real time systems, parallel and distributed systems, grid computing, sensor networks, and robotics.

Besada Adeeb Anees obtained his B.Sc. degree from Menoufia University in 1977 in the Electronics Department and his M.Sc in the field of control in 2006 from Helwan University. He is currently working in his PhD scheme in the field of Artificial Muscles. His research interests include control systems, Fuzzy logic, neural networks, swarm based control.